AGU PUBLICATIONS

JGR

Journal of Geophysical Research: Atmospheres

RESEARCH ARTICLE
10.1002/2015JD024508

Key Points:
- Droplet size-dependent fog chemistry
- Smaller fog droplets contain more oxidized organics than larger droplets
- Important role of transition metals revealed by model

Supporting Information:
- Supporting Information S1

Correspondence to:
T. Gupta and S. N. Tripathi,
tarun@iitk.ac.in;
snt@iitk.ac.in

Citation:
Chakraborty, A., B. Ervens, T. Gupta, and S. N. Tripathi (2016), Characterization of organic residues of size-resolved fog droplets and their atmospheric implications, *J. Geophys. Res. Atmos.*, *121*, 4317–4332, doi:10.1002/2015JD024508.

Received 14 NOV 2015
Accepted 18 APR 2016
Accepted article online 20 APR 2016
Published online 30 APR 2016

Characterization of organic residues of size-resolved fog droplets and their atmospheric implications

Abhishek Chakraborty[1], Barbara Ervens[2,3], Tarun Gupta[1,4], and Sachchida N. Tripathi[1,4]

[1]Department of Civil Engineerin, Indian Institute of Technology, Kanpur, India, [2]CIRES, University of Colorado, Boulder, Colorado, USA, [3]NOAA, ESRL/CSD Boulder, Colorado, USA, [4]Centre for Environmental Science and Engineering, Indian Institute of Technology, Kanpur, India

Abstract Size-resolved fog water samples were collected in two consecutive winters at Kanpur, a heavily polluted urban area of India. Samples were analyzed by an aerosol mass spectrometer after drying and directly in other instruments. Residues of fine fog droplets (diameter: 4–16 μm) are found to be more enriched with oxidized (oxygen to carbon ratio, O/C = 0.88) and low volatility organics than residues of coarse (diameter > 22 μm) and medium size (diameter: 16–22 μm) droplets with *O/C* of 0.68 and 0.74, respectively. These O/C ratios are much higher than those observed for background ambient organic aerosols, indicating efficient oxidation in fog water. Accompanying box model simulations reveal that longer residence times, together with high aqueous OH concentrations in fine droplets, can explain these trends. High aqueous OH concentrations in smaller droplets are caused by their highest surface-volume ratio and high Fe and Cu concentrations, allowing more uptake of gas phase OH and enhanced Fenton reaction rates, respectively. Although some volatile organic species may have escaped during droplet evaporation, these findings indicate that aqueous processing of dissolved organics varies with droplet size. Therefore, large (regional, global)-scale models need to consider the variable reaction rates, together with metal-catalyzed radical formation throughout droplet populations for accurately predicting aqueous secondary organic aerosol formation.

1. Introduction

Fog is a cloud whose base is near the Earth's surface with liquid water contents (LWC) ranging between 0.01 and 0.5 g m^{-3} and which results in severe visibility degradation. It is a natural meteorological phenomenon that occurs throughout the world and lasts for few hours to several days. Although fog can act as an effective and natural cleansing agent for air pollutants, several studies around the world have reported a link between air pollution and fog formation [*Kokkola et al.*, 2003; *Tiwari et al.*, 2011; *Syed et al.*, 2012]. Field studies at various locations on both bulk and size-resolved chemical composition of fog water have been conducted [*Collett et al.*, 1999; *Raja et al.*, 2008; *Ehrenhauser et al.*, 2012; *Herckes et al.*, 2014] along with studies on its effects on physicochemical aerosol properties, such as size distribution, chemical composition, and elemental ratios [*Das et al.*, 2008; *Ge et al.*, 2012]. The majority of the earlier studies focused on inorganics present inside fog water [*Munger et al.*, 1983; *Pandis et al.*, 1990; *Forkel et al.*, 1995; *Hoag et al.*, 1999]. Some of these studies also reported droplet size-resolved fog chemistry for inorganics, mainly sulfate [*Hoag et al.*, 1999]. However, several recent field and modeling studies focused on organic fog water constituents [*Kiss et al.*, 2001; *Mazzoleni et al.*, 2010; *Ervens et al.*, 2013; *Herckes et al.*, 2013, 2014]. Organics in fog may originate from dissolution of condensation nuclei, from dissolution of organic trace gases, or from the formation of secondary organic aerosol (SOA) in fog water by aqueous phase chemical reactions (aqSOA) [*Ervens et al.*, 2011; *Kaul et al.*, 2011; *Ge et al.*, 2012]. Such reactions can occur in all aqueous media in the atmosphere, i.e., in cloud, aerosol, and fog water [*Ervens et al.*, 2011], but in the current study, we focus on the latter, while most of the findings can easily be extended to cloud water. Oxidized organics produced via aqueous processing often have different physicochemical properties as compared to traditional gas phase SOA in terms of O/C ratio, hygroscopicity, optical properties, and atmospheric lifetime [*Ervens et al.*, 2011], and, therefore, they likely interact differently with solar radiation (direct/indirect aerosol effects) [*Ervens et al.*, 2011; *Yu et al.*, 2014]. SOA formation in the aqueous phase can occur by both oxidative and nonoxidative processes [*Ervens et al.*, 2011; *McNeill*, 2015], whereas the oxidative processes often lead to highly oxidized products with higher O/C ratios than observed from gas phase reactions. Such highly oxidized products might partly explain the reasons for more highly oxidized SOA in the ambient atmosphere than found in (dry) smog chamber experiments [*Hallquist et al.*, 2009; *Ervens et al.*, 2011; *Lin et al.*, 2014; *Ervens*, 2015; *Herrmann et al.*, 2015;

McNeill, 2015]. To date, very few studies reported elemental ratios (O/C and H/C) of dissolved organic matter (DOM) in bulk fog/cloud water samples [*Mazzoleni et al*., 2010; *Zhao et al*., 2013b]. Elemental ratios can be a measure of aerosol properties, such as cloud condensation nuclei activity [*Jimenez et al*., 2009] and optical properties [*Lambe et al*., 2013]. Since fog contains droplets of different sizes with vastly different LWC and types and concentrations of organics [*Ervens et al*., 2003b], conclusions on aqueous processing based on bulk fog water samples may not result in reliable estimates of the effects of aqueous phase processing on organic aerosols (OA) composition and elemental ratios. In addition to uncertainties associated with such bulk approaches, accurate estimates of the radical concentrations in the aqueous phase are needed to properly understand the extent and impact of aqueous processing on OA oxidation. The role of transition metals (e.g., Cu, Fe, and Mn) in producing aqueous phase OH radicals via Fenton reactions [*Ervens et al*., 2014] in the ambient atmosphere and its subsequent effects on aqSOA formation has been the subject of only a few studies.

Conclusions on the extent of aqueous phase processing can be drawn from modification of aerosol bulk properties upon fog dissipation such as increased WSOC (water-soluble organic carbon) and SOA masses [*Ge et al*., 2012], correlations of O/C with RH (relative humidity) [*Ervens et al*., 2011; *Chakraborty et al*., 2015], presence of tracer compounds such as organosulfur compounds [*Munger et al*., 1986; *Dall'Osto et al*., 2009], or modification of the aerosol size distributions [*Maria et al*., 2004]. The fraction of material that remains in the particle phase upon fog evaporation depends on its volatility. Oxidation usually leads to products with lower volatility [*Jimenez et al*., 2009], but ultimately, oxidation might lead to fragmentation of the carbon backbone and to evaporation of high-volatility products to the gas phase [*Kroll et al*., 2009; *Daumit et al*., 2014].

The volatility is an essential property of organic aerosol constituents, and organic aerosol models apply so-called "volatility bins" in order to classify classes of organics and their partitioning behavior between the gas and particulate phases [*Lane et al*., 2008; *Grieshop et al*., 2009; *Murphy et al*., 2012]. Volatility is often measured using a thermodenuder where particles are exposed to different temperatures in order to determine their vaporization enthalpy [*An et al*., 2007].

No previous fog-related field study has explored the volatility of size-resolved fog droplet residues in detail. However, a few studies reported an increase in the O/C ratio of bulk OA and increased oxidized OA and polycyclic aromatic hydrocarbon concentrations from before- to after-fog events and speculated that fog-processed residues with relatively lower volatility probably resulted from these changes [*Ehrenhauser et al*., 2012; *Ge et al*., 2012; *Chakraborty et al*., 2015].

The present study location (Indo-Gangetic Plain (IGP), Kanpur, India) is an ideal place to study the composition of polluted fog water and aqSOA formation via aqueous processing of ambient aerosols due to the combination of severe air pollution and radiation fog events during every winter [*Kaul et al*., 2011]. These fog events last for several hours predominantly during nighttime (usually 22:00 h to 08:00 h but sometimes until noon). Although numerous field studies have previously reported fog water composition, this is the first study that reports the observation of fog droplet size-dependent O/C ratios and volatility of DOM. These observations are accompanied by model studies that use observed data as input values and explore the role of Fenton reactions for OH production in the droplets to reproduce trends in observed O/C ratios as a function of droplet size.

2. Materials and Methods

2.1. Fog Water Sampling

The fog water samples were collected from December to February during the winters of 2012–13 and 2013–14, at the IIT Kanpur (Indian Institute of Technology Kanpur). Kanpur (26.4607°N, 80.3334°E) is located in the center of the Indo-Gangetic Plain (IGP) region and is a large urban environment with a population of ~4.5 million inhabitants [*Mishra and Tripathi*, 2008; *GOI*, 2011]. The main pollution sources in the region are industries, domestic fuel combustion, vehicular transport [*Behera and Sharma*, 2010], and biomass burning, which contribute up to 31% of submicron OA [*Chakraborty et al*., 2015]. IIT Kanpur is located 8 km from the city center but within the boundary of the city. A three-stage Caltech Active Strand Cloud Collector (CASCC)[*Raja et al*., 2008; *Kaul et al*., 2011] with 50% cutoff diameters of 22 μm, 16 μm, and 4 μm

[*Kaul et al*., 2011] from the first to third stages, respectively, was used to collect droplet size-resolved fog water samples. In this study stage cutoff diameters are taken as diameters for coarse (C), medium (M), and fine (F) droplets. For each fog event, all three droplet size classes were collected simultaneously. On average, coarse, medium, and fine droplets represented 38%, 42%, and 20% of the total fog LWC, respectively.

The fog water collector and cloud combination probe Droplet Measurement Technologies (DMT) placed at the roof of the building, housing other instruments such as an aerosol mass spectrometer (AMS, Aerodyne Inc.) and a Vaisala relative humidity (RH) and temperature sensor. RH varied from 92 to 100% during fog events with an average of 97%, while temperature varied from 2 to 10°C. After each fog event, fog water collectors were cleaned by rinsing them with high-purity deionized water ($\rho > 18\,M\Omega\,cm$), and field blanks were collected routinely to ensure the adequacy of the collector-cleaning procedures. Average field blank values are shown in Table S1 in the supporting information (SI). In total, 70 fog water samples were collected, out of which four could not be analyzed due to their extremely low volume (<5 mL). The remaining 66 samples were analyzed by AMS, but due to volume limitations, the number of samples actually analyzed in other instruments were limited. Out of 66 samples, 37 were coarse, 15 were medium, and 14 were fine droplet samples. Differences in LWC of droplet classes and variability in the maximum number of collecting bottles allotted for different stages (three for coarse and one each for medium and fine droplets) resulted in different numbers of samples for different droplet sizes. We have considered three collecting bottles of the first stage as different samples, which resulted in a higher number of coarse droplet samples. This may result in some differences in the exact cut points of the collected samples as the foremost collecting strands of the first stage may sample slightly larger sizes of droplets than the last strand of the same stage. However, results showed no significant differences among those coarse droplet samples collected during a single event; therefore, the composition of fog water in a particular size class for each fog event was assumed to be very consistent. Immediately after collection, fog water samples were filtered through a 0.22 μm membrane filter to remove any suspended particles. Due to this instrumental limitation, the discussion in the current study is restricted to the soluble fraction of fog water samples. Filtering of fog water samples was necessary to prevent clogging of the atomizer, the inlet of the AMS, and other instruments, although in doing so some undissolved/insoluble part of organic matter (OM) was lost. Other fog studies have shown that this fraction might comprise up to 25% of the total OM [*Herckes et al*., 2002, 2013]. However, the lost insoluble materials is unlikely to be processed by fog as it is not dissolved in fog droplets and thus does not take part in aqueous phase reactions inside the droplets.

The whole process from fog water collection to storage was usually completed within 10 min. After filtration, samples were deep frozen at −20°C in dark in polypropylene bottles until further analysis.

2.2. AMS Measurements

Real-time submicron ambient aerosol sampling using the AMS [*DeCarlo et al*., 2006; *Canagaratna et al*., 2007] was carried out simultaneously with fog water sample collection via the fog water collector (for details, see *Chakraborty et al*. [2015]). The AMS inlet lenses have 100% particle transmission efficiency from 70 to 700 nm and partial transmission for particle diameters from 700 nm to 1.5 μm [*Takegawa et al*., 2005; *DeCarlo et al*., 2006; *Canagaratna et al*., 2007; *Liu et al*., 2007]. Therefore, the AMS inlet cutoff size does not allow direct sampling of fog water droplets, but it can sample residual ambient aerosols, such as droplet residues upon evaporation during a fog event [*Ge et al*., 2012; *Gilardoni et al*., 2014; *Chakraborty et al*., 2015]. For offline analysis of fog water samples via AMS and AMS + TD (thermodenuder), the samples were atomized by a commercial TSI atomizer (Model 3079), using particle-free compressed zero air. The AMS was operated with a silica gel drier in front of the sampling line (outlet RH < 20%) during ambient and lab-based fog water studies to prevent direct entry of moisture into the instrument. Therefore, the AMS characterization of fog water samples presented in the current study indicates the characteristics of fog droplet processed aerosol residues, which remained in the particle phase after droplet water evaporation in the silica gel drier. However, during drying, small, highly oxidized, volatile organics, such as formaldehyde, or formic acid, can also be removed together with the evaporating water. This removal of small volatile organics occurs from fog water samples of every droplet size, so our relative comparison of the composition of droplet residues remains unaffected due to the loss of these species. These species evaporate under ambient conditions as well, so conclusions drawn in this study about the changes in composition of ambient organic aerosol due to fog processing are meaningful. During real-time ambient sampling, the AMS also sampled submicron background interstitial ambient aerosols present at the site before or during a fog event, which were too small and/or

too hydrophobic to be activated into fog droplets. Generally, condensation nuclei for fog droplets are a fraction of the submicron aerosol population with activated fractions of <20–100%, depending on particle size [*Frank et al*., 1998; *Patidar et al*., 2012; *Hammer et al*., 2014]. Therefore, real-time ambient submicron AMS data and offline fog water AMS data can be compared to understand the extent of aqueous processing of organics inside fog droplets. However, only soluble organic fractions in fog water are characterized here, which are generally more oxidized (higher O/C) than insoluble and/or less hygroscopic organics [*Ervens et al*., 2013; *Timonen et al*., 2013; *Xu et al*., 2015], whereas in real-time mode, AMS sampled total ambient OA, including insoluble, less oxidized, and less hygroscopic organics. Therefore, the O/C ratio of drop residues might be somewhat biased high in comparison to the real-time ambient OA. For clarity, in the current study, we refer to in situ online AMS sampled, submicron ambient OA (background/interstitial/residual) as "ambient OA" and to soluble organics in drop residues obtained from offline AMS analysis as "residual OM."

The AMS was only operated in V mode due to its higher sensitivity, and obtained high resolution (HR) data were processed using PIKA (v1.10H) in IgorPro [*Aiken et al*., 2008]. AMS calibration for calculating ionization efficiency was carried out before and after the analysis of fog water samples by atomizing pure NH_4NO_3 particles of 350 nm diameter. In addition to that, pure $(NH_4)_2SO_4$ was also analyzed in the AMS, in order to determine different sulfate fragment ratios.

2.3. AMS/TD Measurements

For the combined AMS/TD measurements, the atomized aerosols were passed through the drier and TD (kept at 200°C) to the AMS. The TD was built in-house with a 1 m heating section and having a 1 cm internal diameter; aerosol residence time (RT) inside the TD was 53 s. This residence time is on the higher side as compared to usual TD analysis in the literature, but the higher residence time may also help the system to reach equilibrium inside the TD [*An et al*., 2007]. Since our main objective is the comparison among different droplet sizes, our conclusions do not strongly depend on experimental parameters, such as TD losses (around 12%) and RT (53 s), as we maintained the same setup for all droplet sizes.

Several studies in the past have also deployed similar setups involving an atomizer for offline chemical analysis of cloud water and filter extracts using AMS [*Crilley et al*., 2013; *Kaul et al*., 2014; *Canagaratna et al*., 2015]. The deployed commercial atomizers can produce a very high number of particle concentrations ($> 10^5$ cm^{-3}) and consume very little sample volume (0.1 cm^3 min^{-1}) [*Joshi et al*., 2012; *Kaul et al*., 2014]. Atomized fog water samples were first passed through a silica gel-based diffusion drier (outlet RH < 20%) and then to the AMS for 30 min per sample. Some of the samples were analyzed twice to test reproducibility, which was found to be excellent as values of each parameter (mass concentrations, O/C, f44) were within 5%. The AMS is designed for online sampling; fog water samples were analyzed offline via atomization; therefore, AMS mass concentrations for different chemical species (OM, nitrate, sulfate, chloride, and ammonium) in fog water samples may not represent true ambient "air" concentrations. However, this is a comparative study among different droplet sizes, and general trends of species concentrations across the droplet sizes can be compared from AMS results. From the AMS results, we also obtained the elemental ratios of organic matter (OM) present in the fog water residues, and as these are normalized parameters, they are independent of the type of analysis (online or offline).

2.4. Metal and Total Water Soluble Organic Carbon Analysis

Metal analysis was carried out by Thermo Scientific ICP-OES (Inductively Coupled Plasma Optical Emission Spectrometer, ICAP 6300 Thermo, Inc.). This instrument uses superheated Argon plasma of 7000–10,000 K to break down and excite the atoms of the different elements and then identifies the elements from the characteristic wavelength emitted during the relaxation process after atom excitation. It is a fairly rapid process and can identify up to 60 elements simultaneously. The instrument was calibrated using a multielement standard, and samples were blank corrected. For Cu and Fe measurements the ICP-OES has a detection limit of 2.4 and 3 ppb with 9% and 12% uncertainty, respectively. Since this technique detects the total amount of Fe and Cu ions [*Brennan*, 2008], a fraction of which is likely unavailable for chemical reactions due to formation of metal organo complexes or salts and/or acting as a chelating agent, the assumption of all metal ions being available for aqueous phase chemistry is likely an overestimate (section 4.1).

For the determination of WSOC concentrations in fog water, samples were analyzed in a Shimadzu total organic carbon (TOC) analyzer (Shimadzu TOC-V 5500/TNM-1, Kyoto, Japan). TOC standards were prepared

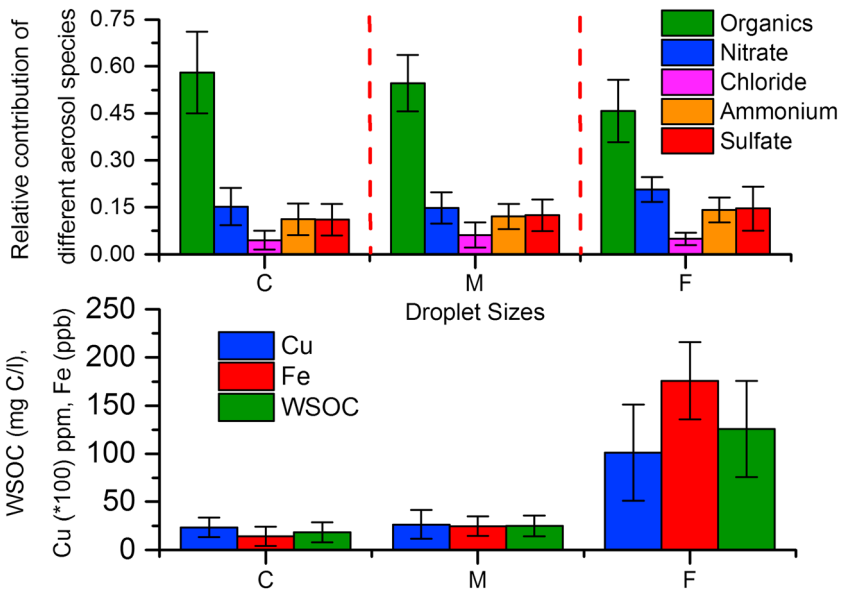

Figure 1. Overall droplet size-segregated fog water composition of coarse (C), medium (M), and fine (F) droplets. Relative contributions of different aerosol species in fog water residues are derived from AMS data by dividing each species mass concentration by the total ($Org + NH_4 + NO_3 + SO_4 + Cl$) mass concentration. Error bars represent ±1 standard deviation.

from a reagent grade potassium hydrogen phthalate diluted with Milli-Q water. TOC concentrations were calculated with the instrument software, and a five-point standard calibration curve that ranged from 0.05 to 200 mg/L was generated. The limit of detection was based on 3 times the standard deviation of blanks (0.06 mg/L of C) with 9% measurement uncertainty. WSOC values also increased with decreasing droplet sizes, similar to the AMS-measured fog water DOM trend (Figures S1 and 1).

3. Results and Discussions

3.1. Overall Composition of Fog Water Residues

The overall composition of droplet residues for all three droplet sizes, as obtained from offline AMS analysis, is dominated by organics (Figure 1), but the organic fraction decreases from coarse to fine droplet residues (59% to 44%, respectively). The decrease is statistically significant with $p < 0.01$. The reason for this is not fully clear but may be caused by the differences in the chemical composition of the condensation nuclei, dominance of fragmentation as oxidation mechanism for highly oxidized residual OM present in fine droplets, which leads to the loss of organic mass (carbon) [*Kroll et al*., 2009; *Daumit et al*., 2014], and/or by the larger surface-to-volume ratio of the smaller droplets that facilitates the increased uptake of OH radicals that might lead to continuous oxidation of organic compounds, which ultimately might result in volatile products [*Ervens et al*., 2003b, 2014].

WSOC mass as measured by the TOC analyzer of filtered fog water samples is much higher in fine droplets (126 mgC/L, Figure 1) than in the coarse and medium ones (19 and 24 mgC/L, respectively). The range of WSOC values varied from 7 to 209 mgC/L, which is well within the range of values (10–280 mgC/L) reported for polluted fogs around the world [*Herckes et al*., 2013].

From coarse to fine droplets, the transition metal concentrations increased significantly; from 0.23 to 1 ppm for Cu and from 0.01 to 0.18 ppm for Fe, respectively (Figure 1). The highest relative contributions from sulfate (15%) and nitrate (21%) are also observed in fine droplet residues. In some previous studies, sulfate was associated with larger droplets that have the highest LWC [*Pandis et al*., 1990; *Moore et al*., 2004a], but in this case it seems that the higher surface-to-volume ratio, longer residence time in the atmosphere, and/or higher metal concentrations of fine droplets may have outweighed the lower LWC. In this location, fog water is more enriched in nitrate than in sulfate, because ambient NO_x levels are much higher than SO_2 levels with average mixing ratios during winter time of 4.4 ppbv and 1 ppbv for NO_x and SO_2, respectively [*Sinha et al*., 2014].

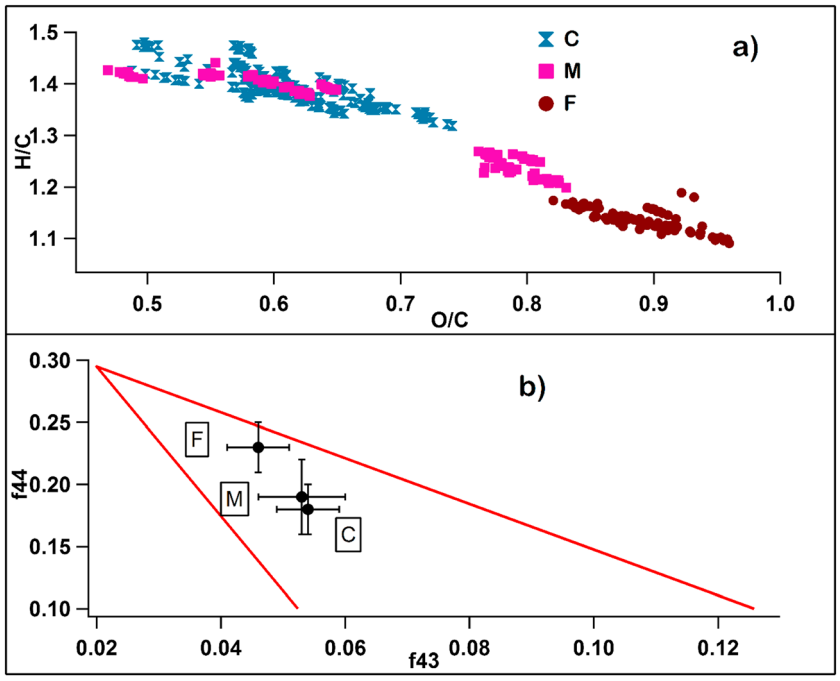

Figure 2. (a) Measured H/C and O/C ratios for fine (F), medium (M), and coarse (C) droplets. (b) Average f44 [(*m/z* 44)/total OA] and f43 [(*m/z* 43)/total OA] signals for the three droplet classes. Red lines show the "triangle plot" for ambient OA as suggested by *Ng et al*. [2011]. Error bars denote ±1 standard deviation.

The fog water pH indicated slightly acidic or neutral solutions ($5.1 < pH < 7.3$) and did not vary much across droplet sizes. NH_4^+ concentrations were sufficient to neutralize the acidic anions (SO_4^{2-}, NO_3^-) in all three droplet sizes.

Fine droplet residuals also contain the highest concentrations of all aerosol constituents, as expected (Figure S1), since they are least dilute. Fine droplet samples result in a visibly "yellowish" solution compared to almost clear solutions of other drop sizes (Figure S2). The presence of light-absorbing materials in fog and cloud water has been reported before in locations impacted by biomass burning [*Gelencser et al*., 2003; *Nguyen et al*., 2012; *Desyaterik et al*., 2013].

Generally, for all solutes, intradroplet variability (Figure 1) was significant across all three droplet sizes, which indicates that the composition of droplet residues from similar droplet size fractions also show considerable variation from one fog event to another.

3.2. Characteristics of Organic Residues of Size-Resolved Droplet

3.2.1. O/C Ratio

AMS-derived O/C ratios of size-resolved fog droplet residues (average of all samples O/C = 0.73) are much higher than those of ambient submicron OA, present before or during the fog (O/C ~ 0.40 and 0.54, respectively) [*Chakraborty et al*., 2015]. The O/C ratios of fine droplet residues are also much higher than those of the other two coarser droplet size residues, while their H/C ratio is much lower (H/C = 1.15) compared to residual OM associated with larger droplets (H/C =1.33 and 1.29 for coarse and medium droplets, respectively; Figure 2a). This indicates that fine droplet residues contain more highly oxidized OM than coarse or medium droplet residues. This observation is further supported by the dominance of more oxidized functional groups like carboxylic acids in fine droplet residues ([CHOgt1 (O > 1)], organic fragments in AMS containing more than one oxygen in Figure S3) compared to the larger size droplet residues, where CH groups from less oxidized organic compounds dominate [*Frossard et al*., 2014]. In terms of the O/C ratio, WSOC mass, and OM functional group composition, coarse and medium droplet residues are very similar; the reason for these similarities between coarse and medium droplet residues can be attributed to similarities in their LWC as described in section 2.1. In the case of medium droplet residues, a clear split is observed in their O/C ratio,

ranging from moderate to higher O/C (Figure 2a). The reason for this trend is not fully clear; future investigations to explain this observation with a higher number of samples of fog water are warranted.

In the present study, the average O/C ratios of fog water residual organics for all three droplet classes are much higher than the values reported in other studies for bulk fog and cloud water (O/C = 0.43 and 0.62, respectively) [*Mazzoleni et al*., 2010; *Zhao et al*., 2013b]. However, in those studies, fog water samples are directly analyzed via the soft ESI (electro spray ionization) technique without any prior drying, so some differences may have been caused by the analysis of the different media (fog water versus residues) and different methods of analysis (hard electron impact ionization in AMS versus soft ESI technique). A large fraction of dissolved fog water OC is usually composed of small volatile organic acids and aldehydes, e.g., HCHO and HCOOH [*Ervens et al*., 2013; *Herckes et al*., 2013], which largely evaporate during water evaporation [*Daumit et al*., 2014] while passing through the silica gel drier in front of the AMS and, therefore, are unlikely to contribute to the fog residue O/C. However, the residual + interstitial ambient OA during fog events also had much lower average O/C ratio (0.54) than the fog water organic residues (average O/C = 0.73) but exhibited a higher ratio than prefog ambient OA (average O/C ~ 0.4, range: 0.30–0.60). However, as mentioned earlier, ambient OA consists of both more oxidized water-soluble and less oxidized nonsoluble organics, while fog droplet residues only represent the soluble fraction of OM. Therefore, it is important to identify whether these higher O/C ratios inside fog droplets have resulted from scavenging of water-soluble, highly oxidized organics from ambient OA or whether oxidative processing occurred on organics inside the droplets. Unfortunately, characteristics of water-soluble organics of ambient OA have not been separately measured. However, oxidized ambient OA can be considered to be a proxy of WSOA (water-soluble OA) [*Timonen et al*., 2013], so using source apportionment of ambient OA, one can separate out the oxidized (secondary) OA from total ambient OA, thus, indirectly quantifying the WSOA contribution to total OA. Based on source apportionment of ambient OA [*Chakraborty et al*., 2015], OOA, i.e., oxidized OA and aged biomass burning OA (BBOA) factors have been identified, which are both secondary or atmospherically processed OA with much higher O/C ratio in addition to several primary factors, i.e., HOA (hydrocarbon-like OA, which mostly originates from vehicular emissions) and BBOA. Based on this previous analysis, we have calculated the bulk O/C ratio of prefog WSOA (section 1 and Figure S4 in Supporting Information S1) and found it to be much higher (O/C = 0.60) than the O/C ratio of prefog ambient total OA (O/C = 0.47) but even lower than the average O/C value of least oxidized coarse droplet residues (O/C = 0.68). This suggests that aqueous oxidation has occurred inside the droplets leading to an enhancement of the O/C ratio. This enhancement is also reflected in trends of the O/C ratio of ambient OA as it increased from prefog to postfog periods (Figure S5).

These findings could have important implication for smog-fog-smog cycle proposed by *Munger et al*. [1983]. Highly oxidized and possibly more hygroscopic fog residues [*Asa-Awuku et al*., 2015] can interact more efficiently with atmospheric moisture, thus paving the way for more smog and fog formation under suitable meteorological conditions. The addition of these highly oxidized fog-processed residues to preexisting aerosols increases their soluble mass and therefore may lead to higher drop numbers during a fog event. In a previous aerosol volatility study, it was found that fine droplet residues contain more low volatility OM than coarser ones, in line with their higher O/C ratios (cf. also section 3.2.3) [*Jimenez et al*., 2009]. However, the volatility and O/C relationship is very complex, and higher O/C does not always lead to lower volatility as reported in a few previous studies [*Tritscher et al*., 2011; *Paciga et al*., 2016]. Volatility can be influenced by several other parameters like carbon number, molecular structures, and ambient conditions [*Kroll et al*., 2011; *Tritscher et al*., 2011; *Donahue et al*., 2014; *Paciga et al*., 2016].

3.2.2. Triangle Plot

In order to elucidate the difference further among residues of differently sized fog droplets, the f44 versus f43 triangle plot [*Ng et al*., 2011] is used (Figure 2b). In this plot, f44 denotes the mass of ($m/z = 44$)/total OA and f43 is the mass of ($m/z = 43$)/total OA. In the AMS, $m/z = 44$ usually originates from the decarboxylation of organic acids [*Takegawa et al*., 2005; *Zhang et al*., 2005], while $m/z = 43$ is from fragmentation of less oxidized aldehydes and ketones [*Miyakawa et al*., 2008]. As OA aging continues, f44 typically increases, whereas f43 decreases indicating the conversion of less oxidized aldehyde or ketone functional groups to more oxidized carboxylic functional groups, thus, causing a shift of the data points toward the upper left corner in the triangular space. This triangle plot also reveals that the fine droplet residues contain more aged and oxidized OM than the residues of the other two droplet sizes. There are several explanations for this trend: (i) Fine droplets have a higher surface-to-volume ratio than larger ones which allows faster dissolution of small carbonyls that

might act as aqSOA precursors in those droplets [*Ervens et al*., 2003b]. (ii) Not only the uptake rates of organic compounds but also those of oxidants (e.g., OH radicals) are enhanced, which leads to more efficient oxidation of aqSOA precursors [*Ervens et al*., 2014]. (iii) The concentration of Fe and Cu ions is many times higher inside fine droplets than in coarser ones (Figure 1), possibly leading to additional OH radical production but also to other complex interactions in terms of organic ligand chemistry and other oxidant cycling. However, the effects associated with metal chemistry cannot be fully quantified here due to the lack of complete information of their dissolved fraction in fog water (cf. section 4). (iv) The ambient residence time of fine droplets can be expected to be generally higher (slower settling) as compared to larger droplets, so organics inside the fine droplets might be processed for longer duration. (v) It is possible that fine and coarse droplets have formed on condensation nuclei with different composition [*Gupta et al*., 2004; *Singh et al*., 2011]. It seems likely that all of these reasons might have contributed to the observed trends to some extent; however, based on the current data set, only (i) and (ii) can be considered as more certain, whereas the other ones are rather speculative.

3.2.3. Volatility of Residual OM

Fog water samples were atomized and passed through a silica gel drier and TD kept at 200°C to the AMS to determine the extremely low volatility (ELV) fraction of residual OM. This remaining mass fraction (MFR) is the fraction of the mass of the droplet residues that remains in the particle phase after being heated at 200°C inside the TD. Residues left behind after droplet evaporation are already less volatile than the volatile species that evaporate simultaneously with fog water. However, most of the AMS + TD-based field volatility studies [*Huffman et al*., 2009; *Häkkinen et al*., 2012; *Poulain et al*., 2014; *Gkatzelis et al*., 2016] were conducted on previously dried ambient aerosols (usually inlet RH $< 20\%$) with a wide range of heating temperatures from 50°C to 400°C, and the main aim of those studies was to evaluate the volatility profiles of ambient OA. Results of those studies indicated that the major fraction of the ambient OA is semivolatile in nature [*Huffman et al*., 2009; *Lee et al*., 2010; *Häkkinen et al*., 2012], i.e., it was evaporated at 150–200°C. This means that, depending upon atmospheric conditions, they can be present in the gas or particulate phases, respectively [*Huffman et al*., 2009]. Although ambient particles will never be exposed to 150–200°C, the vaporization enthalpy as determined in the TD allows conclusions about its gas/particle partitioning in the ambient atmosphere.

Therefore, the result of our volatility study provides some indication about the fractions of these droplet size-resolved oxidized residues being ELV or semivolatile in nature. The ELV fraction is more likely to remain in the particle phase under different ambient conditions, whereas the semivolatile fraction may (partially) escape to gas phase during daytime when temperatures are high and ambient concentrations are diluted due to boundary layer expansion. This kind of size-segregated volatility measurement of fog droplet residues has not been carried out before. The relative comparison among the residues of the three droplet sizes demonstrates that fine droplet residues with highest O/C ratios also contain the highest fraction of ELV OM, while coarser droplet residues with lowest O/C ratios contain the lowest fraction. The difference in MFR between coarse (0.35 ± 0.05) and fine droplets (0.43 ± 0.04) is modest in magnitude but statistically significant, $p < 0.03$ (Figure 3a). This result is in agreement with the conventional inverse relationship between OA oxidation ratio and OA volatility [*Jimenez et al*., 2009]. These results also demonstrate that a major fraction of residual OM is semivolatile to moderately volatile in nature. However, a substantial fraction ($>30\%$) of residual OM is most likely to remain in the particulate phase under ambient conditions. Interestingly, the fraction of residual OM left behind after TD treatment with a RT of 53 s is still higher than the MFR reported (0.10–0.20) during nonfoggy periods for ambient OA from several studies at other locations at 200°C and with much shorter RT (10–15 s) [*Huffman et al*., 2009; *Lee et al*., 2010]. The contribution of these highly oxidized residues may impact the bulk properties of total background ambient OA, which is reflected in Figure S5 where postfog (daytime period after a fog event) O/C ratios and oxidized OA concentrations are significantly higher compared to prefog periods. Note that the organics lost inside TD do not include highly volatile species (e.g., HCHO and HCOOH) that evaporate upon fog water evaporation, as the atomized fog water is first passed through a silica gel drier before being heated in TD and analyzed by AMS (section 2.3). However, these compounds are not thought to contribute to ambient residual mass, as in ambient fog they also escape to the gas phase during drop evaporation.

The dominance of semivolatile materials in residual OM in spite of overall high O/C ratios is not entirely surprising considering that laboratory studies suggested that aqueous oxidation can produce organics with a wide range of volatilities, ranging from volatile to extremely low volatility products [*Dennis-Smither et al*., 2014; *Yu et al*., 2014]. For coarse and medium droplet residues, the difference in the O/C ratios due to TD

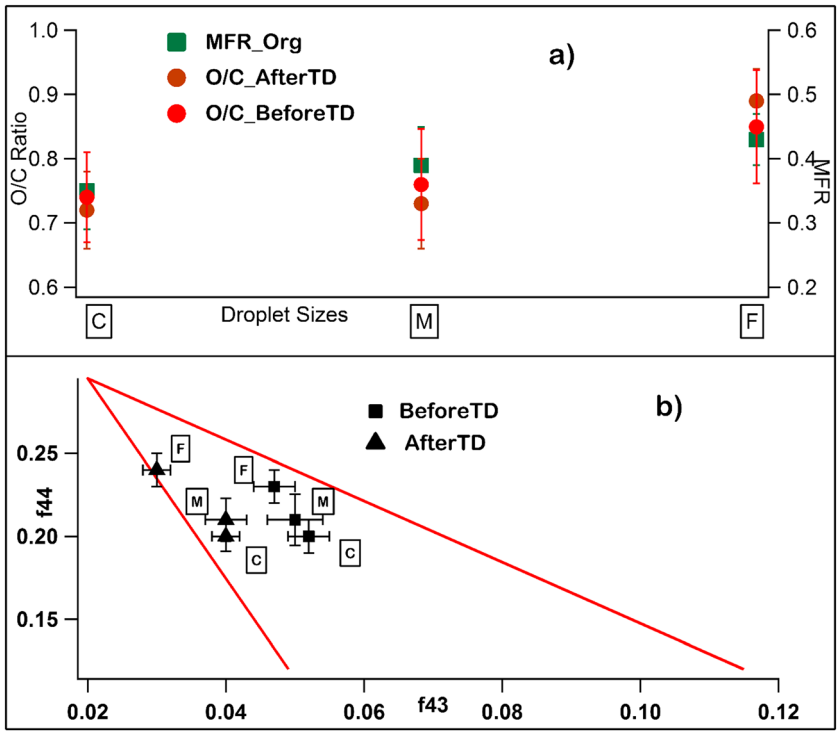

Figure 3. (a) O/C ratio (left axis) and remaining mass fraction (MFR; right axis) and (b) f44 versus f43 in fine (F), medium (M), and coarse (C) droplets before and after passing through a thermodenuder. Error bars represent ±1 standard deviation for each droplet size class.

treatment is insignificant, but for fine droplet residues there is a statistically significant increase ($p < 0.03$); in the triangle plot (Figure 3b), it is observed that only for fine droplets after TD treatment the point moved to the upper left corner, i.e., f44 increased while f43 decreased (both are statistically significant changes, $p < 0.02$), which means that in the fine droplet residues, less oxidized organics are also more volatile in nature.

For large droplet residues, f43 decreases without any corresponding increase in f44 after TD treatment, which is a notable difference to trends for fine droplet residues. Changes in the O/C ratio before and after passing through the TD are also insignificant for large droplet residues. These findings indicate that in coarse droplet residues, the difference in volatility between remaining and evaporated organics cannot be explained by the O/C ratio and/or aging alone. This is not very surprising since several other factors apart from O/C can influence volatility of organics [*Tritscher et al*., 2011; *Paciga et al*., 2016]. In addition, *Altieri et al*. [2008] have shown that higher molecular weight compounds and/or oligomers formed in cloud usually have lower O/C ratios than their monomeric parent compounds but are likely to be less volatile due to a higher number of carbon atoms [*Jimenez et al*., 2009]. Therefore, it seems possible that the remaining, relatively low volatility but less oxidized organics in the coarse droplet residues are oligomers and/or other high-molecular-weight compounds [*Hallquist et al*., 2009].

3.3. OrganoSulfur Compounds as Tracer Compounds for Aqueous Phase Processing

Often, the presence of organosulfur compounds is considered evidence of aqueous processing as they are mostly formed via aqueous chemistry [*Ervens et al*., 2011; *McNeill et al*., 2012]. Organosulfur compounds found in ambient aerosols can comprise organosulfates (OS, $-ROSO_3$) [*Perri et al*., 2010] or sulfonates such as methane sulfonic acid (MSA, CH_3SO_3H) and hydroxyl methane sulfonate (HMS, $HOCH_2SO_3^-$) [*Whiteaker and Prather*, 2003; *Dall'Osto et al*., 2009; *Ge et al*., 2012]. Unambiguous and quantitative identification of any type of organosulfur compounds is very difficult using AMS as it uses a hard thermal decomposition process resulting in complete fragmentation of the parent molecules [*Farmer et al*., 2010; *Hawkins et al*., 2010]. Most of these compounds will be fragmented into smaller SO^+ and SO_2^+ ions, which might be falsely assigned to inorganic sulfates in the AMS fragmentation table [*Hawkins et al*., 2010]. In a previous study, it was concluded based on chamber experiments that some covalent C–O–S bonds of OS may have been

retained inside the AMS even after vaporization, although no OS fragments were directly identified in that study [*Liggio and Li*, 2006]. MSA was qualitatively determined in a previous study of fog-processed ambient residual aerosols using high-resolution (HR) AMS [*Ge et al*., 2012]. *Farmer et al*. [2010] suggested that fragments like $CH_3SO_2^+$ originate from both OS and adducts (sulfonates) in the AMS and can provide an upper estimate of organosulfur compounds present by comparison with organosulfur AMS standards. We observed several organosulfur fragments in HR AMS spectra of fog droplet residuals (Figure S6); the signals of these fragments are clear enough for unambiguous differentiation from adjacent ions. Fragments identified in fog water (Figure S6) match those of methane sulfonic acid (MSA, CH_3SO_3H) in the AMS spectra [*Ge et al*., 2012]. Apart from that, the presence of HMS, considered as another tracer for aqueous processing [*Whiteaker and Prather*, 2003; *Dall'Osto et al*., 2009], is also identified qualitatively via AMS. As HMS formation is generally accelerated at higher pH (>6), the relatively high pH values of collected fog water samples ($5.3 < pH < 7.1$) have provided suitable conditions for HMS formation and stability. The ratio of different sulfate AMS fragments (SO^+/SO_3^+ and SO_2^+/SO_3^+) is higher for samples containing HMS as compared to samples with only ammonium sulfate, since some fragments, such as SO_3^+, are not produced by HMS [*Dall'Osto et al*., 2009; *Ge et al*., 2012]. These ratios (SO^+/SO_3^+ and SO_2^+/SO_3^+) are nearly 2–3 times higher in residual OM (11 and 17, respectively) compared to the ratios observed in ambient OA (5 and 6, respectively) during the study period. These ratios are also much higher than those from pure ammonium sulfate fragments (5 and 7, respectively) determined by our AMS. Therefore, it seems that OS, such as HMS, are present inside fog water residues in significant quantity. We have not analyzed any organosulfur standards in our AMS, so we are unable to provide any quantitative estimates. Interestingly, no organosulfur fragments were identified in AMS spectra of the real-time ambient (background) OA mass taken during the foggy periods of 2012–13 and 2013–14, which strongly suggests that OS were formed in the fog droplets.

4. Trends in aqSOA Formation Predicted by Box Model Studies

4.1. Model Description

In order to explore the reasons for the drop-size-dependent trends in OA loading and oxygenation state, model simulations were performed with a particular focus on the role of OH sources within the droplet. The detailed model description can be found in section 3 of SI, with the initial aqueous phase concentrations in Table S1, uptake parameters in Table S2, and gas phase mixing ratios in Table S3. We do not attempt to exactly reproduce the chemical composition of the fog droplets or their residues due to the lack of detailed gas phase measurements during the study period. Instead, we chose glyoxal as a proxy of aqSOA precursors, since its oxidation chemistry has been studied in detail before [*Lim et al*., 2013], and simulate its oxidation chemistry in fog droplets. This approach is quite simplified and might lead to an overestimate of the resulting O/C ratios as other precursors are known to produce less oxidized compounds. However, a relative comparison between the droplet sizes is still meaningful and reveals sensitivities of trends in O/C ratios to oxidant levels and droplet sizes. The goal of the model studies is to predict trends in oxygenation state (O/C) throughout the drop population and therefore to test our understanding of aqSOA formation and processing within the aqueous phase. Assumptions of O/C ratios of aqSOA products upon glyoxal oxidation are discussed in section 3 of S1.

The three droplet classes in the model are represented by average drop sizes (10, 20, and 25 μm) that are created from averages of the measured droplet populations (Figure S7). OH in the gas phase is initialized with a relatively low concentration ($5 \cdot 10^4\,cm^{-3}$), which corresponds to typical levels as observed during night at other locations, which seems appropriate for the foggy periods that occurred mostly during nighttime and morning hours. These concentrations result in glyoxal concentrations of a few tens of parts per thousand upon oxidation of proxy precursors (toluene, benzene, and isoprene; Table S3) and glyoxal productions rates of <10 ppt/s, being in agreement with prior measurements at various locations [*Washenfelder et al*., 2011].

In a first simulation, it is assumed that all OH in the aqueous phase is transported from the gas phase. The second simulation considers Fenton reactions as an additional OH source and subsequent recycling of the oxidized metal ions via

$$Fe^{2+}/Cu^{+} + H_2O_2 \rightarrow Fe^{3+}/Cu^{2+} + OH^{-} + OH \quad \text{(R1)}$$

$$Fe^{3+}/Cu^{2+} + HO_2/O_2^{-} \rightarrow Fe^{2+}/Cu^{+} + O_2(+H^{+}) \quad \text{(R2)}$$

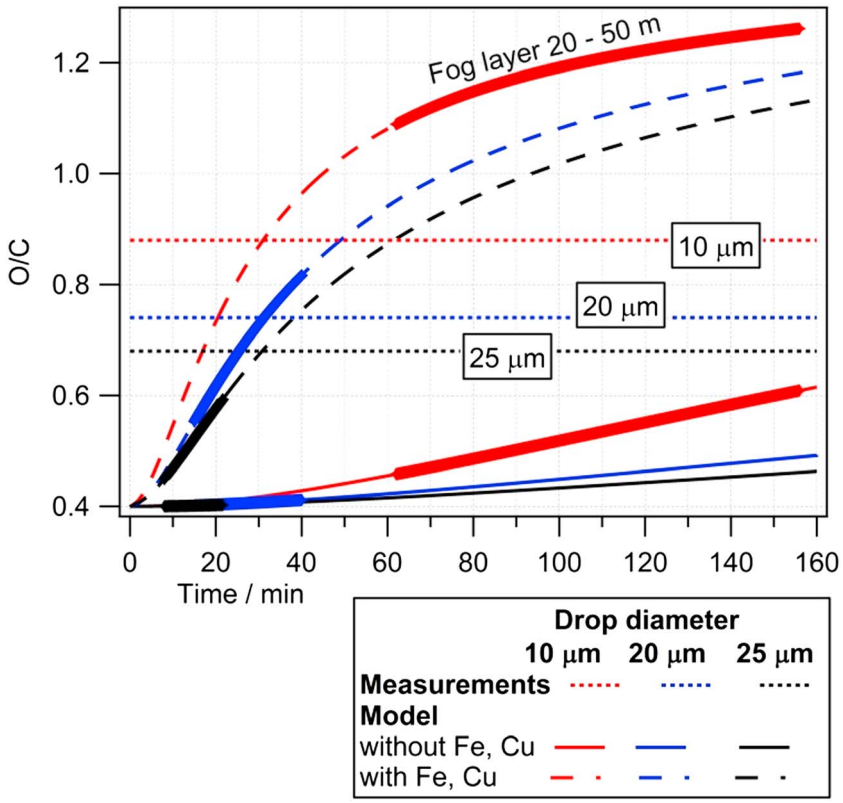

Figure 4. Predicted and observed (dotted lines) average O/C ratios for drop sizes 10 μm (red), 20 μm (blue), and 25 μm (black). Model results are bounded by the assumptions that none (solid lines) or all (dashed lines) Fe and Cu ions are available for photochemical Fenton reactions. Bold lines mark ranges for assumed fog thickness of 20–50 m.

Fe and Cu concentrations for the three drop classes were taken from the fog water measurements (section 2.4). While we assume in the second simulation that all Fe and Cu ions are available for aqueous phase reactions, this assumption might represent an overestimate since not all ions might be dissolved. Previous measurements of the photochemically available fraction of iron in aerosol particles have shown values from <3% to 100% [*Siefert et al.*, 1996]. In fog and stratus clouds, this fraction was on average smaller (2–53%) for iron, whereas it was similar for copper (13–100%) [*Siefert et al.*, 1998]. The model does not include the direct photolysis of metal-organo-complexes (e.g., iron-oxalato complexes). Under particular conditions, these processes might be a substantial sink for oxalate [*Sorooshian et al.*, 2013]; however, for ligands other than oxalate, they will not affect a large fraction of the total OM [*Weller et al.*, 2014].

Previous model sensitivity studies have suggested that under many conditions OH uptake is the main OH source in the aqueous phase, followed by Fenton reactions [*Ervens et al.*, 2003a; *Tilgner et al.*, 2013]. Some studies suggest that additional OH sources in the aqueous phase exist, e.g., from organic compounds [*Zhao et al.*, 2013a]; however, due to the lack of mechanistic data, these sources cannot be quantified to date yet. Due to these canceling effects (i.e., overestimating the role of Fenton reactions and neglecting other OH aqueous phase sources), we think that our assumption of using Fenton reactions as the only chemical OH source is a reasonable approximation of a high limit of OH in the aqueous phase. A recent sensitivity study suggested that OH-initiated aqSOA formation in the aqueous phase is OH-limited since the moderately soluble OH radical is not sufficiently fast transported into the droplets, and aqueous phase OH sources are not efficient enough to compensate the OH loss to organics [*Ervens et al.*, 2014]. In this latter study, it was shown that on a drop-to-drop basis, aqSOA is most efficiently formed in small droplets as they have the highest surface-to-volume ratio and solute concentrations and, therefore, the highest OH concentration and lowest OH limitation, respectively.

4.2. Model Results

The order of O/C ratios in Figure 4 as predicted by the model follows the observed trends (Figure 3a). Droplets of different sizes likely have different lifetimes and therefore processing times. In order to give a trend of such

time scales, in Figure 4, ranges for assumed lifetimes are marked for the different droplet sizes in the fog layer. As the thickness of the fog layers at the measurement location varied, a range of fog thickness is assumed (20–50 m), in agreement with typical values for radiation fogs. The droplet lifetimes were calculated under the assumption that droplets fall from the middle of a fog layer to the ground [*Seinfeld and Pandis*, 2006]. The resulting time is an average value since other droplets fall from the top of layer and will have a longer lifetime, whereas droplets that fall from near the fog base live shorter. These assumptions bound the lifetime of a droplet, and therefore, the time that is available for aqueous phase processing in a very approximate manner. However, in order to estimate trends and due to lack of other means to estimate this time scale, it seems a reasonable approach. Due to the relatively high RH during foggy periods (average RH = 97%, range of 92–100%, associated measurement uncertainty is 5%), faster evaporation of small droplets was likely negligible as compared to their settling.

The predicted O/C ratios using OH uptake as the only OH source are lower than the observed ones for all drop sizes. If chemical OH sources in the aqueous phase are added ("with Fe, Cu" in Figure 4), O/C ratios tend to be overestimated. However, it should be kept in mind that the model only simulates aqSOA formation from glyoxal. The predicted products oxalate and glyoxylate have a much higher O/C ratio (1.5 and 2, respectively) than frequently found for total aqSOA [*Lim et al*., 2010; *Ervens et al*., 2011; *Lee et al*., 2012]. Comparing the relative differences between predicted O/C ratios for the three drop sizes (Figure 4), the simulations without metal ions (solid lines) show that the O/C ratio in the two largest size classes (medium and coarse) are very similar to each other, whereas the smallest one is predicted to exhibit the highest O/C ratio, in agreement with trends in the measurements (Figure 3a). The results suggest that the role of metal ions in producing OH might have been overestimated, in particular for the smallest droplets where incomplete dissolution might be most likely due to lowest LWC. As discussed earlier, assuming that all measured metal ions are available for aqueous phase reactions likely represents an overestimate. However, additional aqueous phase reactions might also lead to OH radicals (e.g., direct photolysis of H_2O_2 and nitrate [*Ervens et al*., 2003a], or organics); however, their role might be relatively small due to low photochemical activity in the morning hours.

The model studies confirm the general trends in O/C ratios of the measurements. Exact agreement in predicted SOA mass and O/C ratios cannot be expected, since we restricted our simulations to oxidation of glyoxal only, whereas in ambient fog droplets and residues many additional organics will contribute to the organic fraction. Comparison of the two simulations (only OH uptake, and additional chemical OH source in the aqueous phase as denoted as "without Fe, Cu" and "with Fe, Cu," respectively, Figure 4) suggests that not only the higher surface-to-volume ratio of the smaller droplets but also trends in metal concentrations that initiate OH formation as well as estimates of processing times are needed to fully represent variability in oxygenation states within a fog droplet population.

5. Atmospheric Implications and Conclusions

Fog water analysis via AMS revealed that fine droplets (diameter: 4–16 μm) are more concentrated in terms of organic and inorganic solutes as compared to medium (16–22 μm) and coarse (>22 μm) ones. Residues of fine droplets are more enriched in more highly oxidized and low volatility OM as evident from their higher O/C ratio and higher mass fraction remaining in the TD as compared to coarser ones. A substantial portion (>50%) of residual organics left behind by evaporated droplets is removed upon heating at 200°C, indicating that much of the highly oxidized residues are semivolatile in nature. However, it also indicates that a decent portion of droplet residues will remain in the particulate phase and possibly impact the properties of background aerosols as evident from the increase in the O/C ratio that occurred during fog events as shown by the comparison of prefog and postfog samples. Accompanying box model studies support that fine droplets can produce much more highly oxidized material than their larger counterparts. Model results also indicate the importance of metal-assisted Fenton reactions in producing highly oxidized OM. Our findings also suggest that to accurately predict SOA formation and processing in fog/cloud droplets and their effects on ambient aerosols, one needs to take into account fog/cloud microstructure, such as droplet size distribution and lifetime, LWC, thickness, and duration. These conclusions are similar to those that were drawn in earlier studies on sulfate formation [*Moore et al*., 2004b].

In South Asia, fog frequency has increased in the last few decades along with air pollution [*Mohan and Payra*, 2009; *Syed et al*., 2012]. Polluted air with more aerosol particles and higher mass loadings usually is more

prone to form fog with more numerous but smaller droplets [*Bréon et al*., 2002; *Pandithurai et al*., 2009]. The smaller drops settle more slowly and thus enhance fog duration and limit cleansing. Therefore, this shift toward smaller fog droplet sizes might lead to enhanced production of highly oxidized, less volatile SOA mass, which in turn might impact the resulting particle properties in terms of hygroscopicity and lifetime. Such trends might (partially) reverse the role of fog as a natural cleansing agent of the atmosphere due to efficient fine particle scavenging and settling of droplets.

Acknowledgments

We acknowledge the support of IIT Kanpur for providing us with an HR-ToF-AMS for PG research and teaching. We would also like to acknowledge support of the Indian Ministry of Human Resource and Development (3-21/2014-TS.1) for providing us some financial assistance to carry out this research. This research is also partially supported by the U.S. Agency for International Development (AID-OAA-A-11- 00012). In addition we thank Deepika Bahttu for useful discussions. All the data and results that are used to support the conclusions of this article can be obtained upon request from the corresponding authors by sending emails to tarun@iitk.ac.in and/or snt@iitk.ac.in. This article contains supporting information of 11 pages (S1–S11) with seven figures (Figures S1–S7) and three tables (Tables S1–S3).

References

Aiken, A. C., et al. (2008), O/C and OM/OC ratios of primary, secondary, and ambient organic aerosols with high-resolution time-of-flight aerosol mass spectrometry, *Environ. Sci. Technol.*, *42*(12), 4478–4485, doi:10.1021/es703009q.

Altieri, K. E., S. P. Seitzinger, A. G. Carlton, B. J. Turpin, G. C. Klein, and A. G. Marshall (2008), Oligomers formed through in-cloud methylglyoxal reactions: Chemical composition, properties, and mechanisms investigated by ultra-high resolution FT-ICR mass spectrometry, *Atmos. Environ.*, *42*(7), 1476–1490, doi:10.1016/j.atmosenv.2007.11.015.

An, W. J., R. K. Pathak, B.-H. Lee, and S. N. Pandis (2007), Aerosol volatility measurement using an improved thermodenuder: Application to secondary organic aerosol, *J. Aerosol Sci.*, *38*(3), 305–314, doi:10.1016/j.jaerosci.2006.12.002.

Asa-Awuku, A., A. Sorooshian, R. C. Flagan, J. H. Seinfeld, and A. Nenes (2015), CCN properties of organic aerosol collected below and within marine stratocumulus clouds near Monterey, California, *Atmosphere (Basel)*, *6*(11), 1590–1607, doi:10.3390/atmos6111590.

Behera, S. N., and M. Sharma (2010), Reconstructing primary and secondary components of $PM_{2.5}$ composition for an urban atmosphere, *Aerosol Sci. Technol.*, *44*(11), 983–992, doi:10.1080/02786826.2010.504245.

Brennan, M. C. (2008), *A Practical Approach to Quantitative Metal Analysis of Organic Matrices*, First., Wiley, Sussex.

Bréon, F.-M., D. Tanré, and S. Generoso (2002), Aerosol effect on cloud droplet size monitored from satellite, *Science*, *295*, 834–838, doi:10.1126/science.1066434.

Canagaratna, M. R., et al. (2007), Chemical and microphysical characterization of ambient aerosols with the aerodyne aerosol mass spectrometer, *Mass Spectrom. Rev.*, *26*(2), 185–222, doi:10.1002/mas.20115.

Canagaratna, M. R., et al. (2015), Elemental ratio measurements of organic compounds using aerosol mass spectrometry: Characterization, improved calibration, and implications, *Atmos. Chem. Phys.*, *15*(1), 253–272, doi:10.5194/acp-15-253-2015.

Chakraborty, A., D. Bhattu, T. Gupta, S. N. Tripathi, and M. R. Canagaratna (2015), Real-time measurements of ambient aerosols in a polluted Indian city: Sources, characteristics and processing of organic aerosols during foggy and non-foggy periods, *J. Geophys. Res. Atmos.*, *120*, 9006–9019, doi:10.1002/2015JD023419.

Collett, J. L., K. J. Hoag, D. E. Sherman, A. Bator, and L. W. Richards (1999), Spatial and temporal variations in San Joaquin Valley fog chemistry, *Atmos. Environ.*, *33*(1), 129–140.

Crilley, L. R., G. A. Ayoko, and L. Morawska (2013), Analysis of organic aerosols collected on filters by aerosol mass spectrometry for source identification, *Anal. Chim. Acta*, *803*, 91–96, doi:10.1016/j.aca.2013.07.013.

Dall'Osto, M., R. M. Harrison, H. Coe, and P. Williams (2009), Real-time secondary aerosol formation during a fog event in London, *Atmos. Chem. Phys.*, *9*(7), 2459–2469, doi:10.5194/acp-9-2459-2009.

Das, S. K., A. Jayaraman, and A. Misra (2008), Fog-induced variations in aerosol optical and physical properties over the Indo-Gangetic Basin and impact to aerosol radiative forcing, *Ann. Geophys.*, *26*(6), 1345–1354.

Daumit, K. E., A. J. Carrasquillo, J. F. Hunter, and J. H. Kroll (2014), Laboratory studies of the aqueous-phase oxidation of polyols: Submicron particles vs. bulk aqueous solution, *Atmos. Chem. Phys.*, *14*(19), 10,773–10,784, doi:10.5194/acp-14-10773-2014.

DeCarlo, P. F., et al. (2006), Field-deployable, high-resolution, time-of-flight aerosol mass spectrometer, *Anal. Chem.*, *78*(24), 8281–8289, doi:10.1021/ac061249n.

Dennis-Smither, B. J., F. H. Marshall, R. E. H. Miles, T. C. Preston, and J. P. Reid (2014), Volatility and oxidative aging of aqueous maleic acid aerosol droplets and the dependence on relative humidity, *J. Phys. Chem. A*, *118*(30), 5680–5691, doi:10.1021/jp504823j.

Desyaterik, Y., Y. Sun, X. Shen, T. Lee, X. Wang, T. Wang, and J. L. Collett (2013), Speciation of "brown" carbon in cloud water impacted by agricultural biomass burning in eastern China, *J. Geophys. Res. Atmos.*, *118*, 7389–7399, doi:10.1002/jgrd.50561.

Donahue, N. M., A. L. Robinson, E. R. Trump, I. Riipinen, and J. H. Kroll (2014), Volatility and aging of atmospheric organic aerosol, *Top. Curr. Chem.*, *339*, 97–144, doi:10.1007/128-2012-355.

Ehrenhauser, F. S., K. Khadapkar, Y. Wang, J. W. Hutchings, O. Delhomme, R. R. Kommalapati, P. Herckes, M. J. Wornat, and K. T. Valsaraj (2012), Processing of atmospheric polycyclic aromatic hydrocarbons by fog in an urban environment, *J. Environ. Monit.*, *14*(10), 2566–2579, doi:10.1039/c2em30336a.

Ervens, B. (2015), Modeling the processing of aerosol and trace gases in clouds and fogs, *Chem. Rev.*, *115*(10), 4157–4198, doi:10.1021/cr5005887.

Ervens, B., et al. (2003a), CAPRAM 2.4 (MODAC mechanism): An extended and condensed tropospheric aqueous phase mechanism and its application, *J. Geophys. Res.*, *108*(D14), 4266, doi:10.1029/2002JD002202.

Ervens, B., P. Herckes, G. Feingold, T. Lee, J. L. Collett, and S. M. Kreidenweis (2003b), On the drop-size dependence of organic acid and formaldehyde concentrations in fog, *J. Atmos. Chem.*, *46*(3), 239–269, doi:10.1023/a:1026393805907.

Ervens, B., B. J. Turpin, and R. J. Weber (2011), Secondary organic aerosol formation in cloud droplets and aqueous particles (aqSOA): A review of laboratory, field and model studies, *Atmos. Chem. Phys.*, *11*(21), 11,069–11,102, doi:10.5194/acp-11-11069-2011.

Ervens, B., Y. Wang, J. Eagar, W. R. Leaitch, A. M. Macdonald, K. T. Valsaraj, and P. Herckes (2013), Dissolved organic carbon (DOC) and select aldehydes in cloud and fog water: The role of the aqueous phase in impacting trace gas budgets, *Atmos. Chem. Phys.*, *13*(10), 5117–5135, doi:10.5194/acp-13-5117-2013.

Ervens, B., A. Sorooshian, Y. B. Lim, and B. J. Turpin (2014), Key parameters controlling OH-initiated formation of secondary organic aerosol in the aqueous phase (aqSOA), *J. Geophys. Res. Atmos.*, *119*, 3997–4016, doi:10.1002/2013JD021021.

Farmer, D. K., A. Matsunaga, K. S. Docherty, J. D. Surratt, J. H. Seinfeld, P. J. Ziemann, and J. L. Jimenez (2010), Response of an aerosol mass spectrometer to organonitrates and organosulfates and implications for atmospheric chemistry, *Proc. Natl. Acad. Sci. U.S.A.*, *107*(15), 6670–6675, doi:10.1073/pnas.0912340107.

Forkel, R., W. Seidl, A. Ruggaber, and R. Dlugi (1995), Fog chemistry during EUMAC Joint Cases: Analysis of routine measurements in southern Germany and model calculations, *Meteorol. Atmos. Phys.*, *57*(1–4), 61–86, doi:10.1007/BF01044154.

Frank, G., et al. (1998), Droplet formation and growth in polluted fogs, *Contrib. Atmos. Phys.*, *71*(1), 65–85.
Frossard, A. A., L. M. Russell, P. Massoli, T. S. Bates, and P. K. Quinn (2014), Side-by-side comparison of four techniques explains the apparent differences in the organic composition of generated and ambient marine aerosol particles, *Aerosol Sci. Technol.*, *48*(3), V–X, doi:10.1080/02786826.2013.879979.
Ge, X., Q. Zhang, Y. Sun, C. R. Ruehl, and A. Setyan (2012), Effect of aqueous-phase processing on aerosol chemistry and size distributions in Fresno, California, during wintertime, *Environ. Chem.*, *9*(3), 221–235, doi:10.1071/en11168.
Gelencser, A., A. Hoffer, G. Kiss, E. Tombacz, R. Kurdi, and L. Bencze (2003), In-situ formation of light-absorbing organic matter in cloud water, *J. Atmos. Chem.*, *45*(1), 25–33, doi:10.1023/a:1024060428172.
Gilardoni, S., et al. (2014), Fog scavenging of organic and inorganic aerosol in the Po Valley, *Atmos. Chem. Phys.*, *14*(13), 6967–6981, doi:10.5194/acp-14-6967-2014.
Gkatzelis, G. I., D. K. Papanastasiou, K. Florou, C. Kaltsonoudis, E. Louvaris, and S. N. Pandis (2016), Measurement of nonvolatile particle number size distribution, *Atmos. Meas. Tech.*, *9*(1), 103–114, doi:10.5194/amt-9-103-2016.
GOI (2011), Indian Census 2011. [Available at http://www.census2011.co.in/census/district/535-kanpur-nagar.html.]
Grieshop, A. P., M. A. Miracolo, N. M. Donahue, and A. L. Robinson (2009), Constraining the volatility distribution and gas-particle partitioning of combustion aerosols using isothermal dilution and thermodenuder measurements, *Environ. Sci. Technol.*, *43*(13), 4750–4756, doi:10.1021/es8032378.
Gupta, T., P. Demokritou, and P. Koutrakis (2004), Effects of physicochemical properties of ultrafine particles on the performance of an ultrafine particle concentrator, *Aerosol Sci. Technol.*, *38*, 37–45, doi:10.1080/027868290502272.
Häkkinen, S. A. K., et al. (2012), Long-term volatility measurements of submicron atmospheric aerosol in Hyytiälä, Finland, *Atmos. Chem. Phys.*, *12*(22), 10,771–10,786, doi:10.5194/acp-12-10771-2012.
Hallquist, M., et al. (2009), The formation, properties and impact of secondary organic aerosol: Current and emerging issues, *Atmos. Chem. Phys.*, *9*, 5155–5236, doi:10.5194/acp-9-5155-2009.
Hammer, E., et al. (2014), Size-dependent particle activation properties in fog during the ParisFog 2012/13 field campaign, *Atmos. Chem. Phys.*, *14*(19), 10,517–10,533, doi:10.5194/acp-14-10517-2014.
Hawkins, L. N., L. M. Russell, D. S. Covert, P. K. Quinn, and T. S. Bates (2010), Carboxylic acids, sulfates, and organosulfates in processed continental organic aerosol over the southeast Pacific Ocean during VOCALS-REx 2008, *J. Geophys. Res.*, *115*, D13201, doi:10.1029/2009JD013276.
Herckes, P., T. Lee, L. Trenary, G. G. Kang, H. Chang, and J. L. Collett (2002), Organic matter in Central California radiation fogs, *Environ. Sci. Technol.*, *36*(22), 4777–4782, doi:10.1021/es025889t.
Herckes, P., K. T. Valsaraj, and J. L. Collett (2013), A review of observations of organic matter in fogs and clouds: Origin, processing and fate, *Atmos. Res.*, *132*, 434–449, doi:10.1016/j.atmosres.2013.06.005.
Herckes, P., A. R. Marcotte, Y. Wang, and J. L. Collett (2014), Fog composition in the Central Valley of California over three decades, *Atmos. Res.*, *151*, 20–30, doi:10.1016/j.atmosres.2014.01.025.
Herrmann, H., T. Schaefer, A. Tilgner, S. A. Styler, C. Weller, M. Teich, and T. Otto (2015), Tropospheric aqueous-phase chemistry: Kinetics, mechanisms, and its coupling to a changing gas phase, *Chem. Rev.*, *115*(10), 4259–4334, doi:10.1021/cr500447k.
Hoag, K. J., J. L. Collett, and S. N. Pandis (1999), The influence of drop size-dependent fog chemistry on aerosol processing by San Joaquin Valley fogs, *Atmos. Environ.*, *33*, 4817–4832.
Huffman, J. A., et al. (2009), Chemically-resolved aerosol volatility measurements from two megacity field studies, *Atmos. Chem. Phys.*, *9*(18), 7161–7182.
Jimenez, J. L., et al. (2009), Evolution of organic aerosols in the atmosphere, *Science*, *326*(5959), 1525–1529, doi:10.1126/science.1180353.
Joshi, M., B. K. Sapra, A. Khan, S. N. Tripathi, P. M. Shamjad, T. Gupta, and Y. S. Mayya (2012), Harmonisation of nanoparticle concentration measurements using GRIMM and TSI scanning mobility particle sizers, *J. Nanoparticle Res.*, *14*(12), doi:10.1007/s11051-012-1268-8.
Kaul, D. S., T. Gupta, S. N. Tripathi, V. Tare, and J. L. Collett Jr. (2011), Secondary organic aerosol: A comparison between foggy and nonfoggy days, *Environ. Sci. Technol.*, *45*(17), 7307–7313, doi:10.1021/es201081d.
Kaul, D. S., T. Gupta, and S. N. Tripathi (2014), Source apportionment for water soluble organic matter of submicron aerosol: A comparison between foggy and nonfoggy episodes, *Aerosol Air Qual. Res.*, *14*(5), 1527–1533, doi:10.4209/aaqr.2013.10.0319.
Kiss, G., B. Varga, A. Gelencsér, Z. Krivácsy, Á. Molnár, T. Alsberg, L. Persson, H. C. Hansson, and M. Cristina Facchini (2001), Characterisation of polar organic compounds in fog water, *Atmos. Environ.*, *35*(12), 2193–2200.
Kokkola, H., S. Romakkaniemi, and A. Laaksonen (2003), On the formation of radiation fogs under heavily polluted conditions, *Atmos. Chem. Phys.*, *3*(3), 581–589, doi:10.5194/acp-3-581-2003.
Kroll, J. H., J. D. Smith, D. L. Che, S. H. Kessler, D. R. Worsnop, and K. R. Wilson (2009), Measurement of fragmentation and functionalization pathways in the heterogeneous oxidation of oxidized organic aerosol, *Phys. Chem. Chem. Phys.*, *11*(36), 8005–8014, doi:10.1039/b905289e.
Kroll, J. H., et al. (2011), Carbon oxidation state as a metric for describing the chemistry of atmospheric organic aerosol, *Nat. Chem.*, *3*(2), 133–139, doi:10.1038/nchem.948.
Lambe, A. T., et al. (2013), Relationship between oxidation level and optical properties of secondary organic aerosol, *Environ. Sci. Technol.*, *47*(12), 6349–6357, doi:10.1021/es401043j.
Lane, T. E., N. M. Donahue, and S. N. Pandis (2008), Simulating secondary organic aerosol formation using the volatility basis-set approach in a chemical transport model, *Atmos. Environ.*, *42*(32), 7439–7451, doi:10.1016/j.atmosenv.2008.06.026.
Lee, A. K. Y., K. L. Hayden, P. Herckes, W. R. Leaitch, J. Liggio, A. M. Macdonald, and J. P. D. Abbatt (2012), Characterization of aerosol and cloud water at a mountain site during WACS 2010: Secondary organic aerosol formation through oxidative cloud processing, *Atmos. Chem. Phys.*, *12*(15), 7103–7116, doi:10.5194/acp-12-7103-2012.
Lee, B. H., et al. (2010), Measurement of the ambient organic aerosol volatility distribution: Application during the Finokalia Aerosol Measurement Experiment (FAME-2008), *Atmos. Chem. Phys.*, *10*(24), 12,149–12,160, doi:10.5194/acp-10-12149-2010.
Liggio, J., and S. M. Li (2006), Organosulfate formation during the uptake of pinonaldehyde on acidic sulfate aerosols, *Geophys. Res. Lett.*, *33*, L13808, doi:10.1029/2006GL026079.
Lim, Y. B., Y. Tan, M. J. Perri, S. P. Seitzinger, and B. J. Turpin (2010), Aqueous chemistry and its role in secondary organic aerosol (SOA) formation, *Atmos. Chem. Phys.*, *10*(21), 10,521–10,539, doi:10.5194/acp-10-10521-2010.
Lim, Y. B., Y. Tan, and B. J. Turpin (2013), Chemical insights, explicit chemistry, and yields of secondary organic aerosol from OH radical oxidation of methylglyoxal and glyoxal in the aqueous phase, *Atmos. Chem. Phys.*, *13*(17), 8651–8667, doi:10.5194/acp-13-8651-2013.
Lin, G., S. Sillman, J. E. Penner, and A. Ito (2014), Global modeling of SOA: The use of different mechanisms for aqueous-phase formation, *Atmos. Chem. Phys.*, *14*(11), 5451–5475, doi:10.5194/acp-14-5451-2014.
Liu, P. S. K., R. Deng, K. A. Smith, L. R. Williams, J. T. Jayne, M. R. Canagaratna, K. Moore, T. B. Onasch, D. R. Worsnop, and T. Deshler (2007), Transmission efficiency of an aerodynamic focusing lens system: Comparison of model calculations and laboratory measurements for the Aerodyne Aerosol Mass Spectrometer, *Aerosol Sci. Technol.*, *41*(8), 721–733, doi:10.1080/02786820701422278.

Maria, S. F., L. M. Russell, M. K. Gilles, and S. C. B. Myneni (2004), Organic aerosol growth mechanisms and their climate-forcing implications, *Science*, *306*(5703), 1921–1924, doi:10.1126/science.1103491.

Mazzoleni, L. R., B. M. Ehrmann, X. Shen, A. G. Marshall, and J. L. Collett Jr. (2010), Water-soluble atmospheric organic matter in fog: Exact masses and chemical formula identification by ultrahigh-resolution Fourier transform ion cyclotron resonance mass spectrometry, *Environ. Sci. Technol.*, *44*(10), 3690–3697, doi:10.1021/es903409k.

McNeill, V. F. (2015), Aqueous organic chemistry in the atmosphere: Sources and chemical processing of organic aerosols, *Environ. Sci. Technol.*, *49*(3), 1237–1244, doi:10.1021/es5043707.

McNeill, V. F., J. L. Woo, D. D. Kim, A. N. Schwier, N. J. Wannell, A. J. Sumner, and J. M. Barakat (2012), Aqueous-phase secondary organic aerosol and organosulfate formation in atmospheric aerosols: A modeling study, *Environ. Sci. Technol.*, *46*(15), 8075–8081, doi:10.1021/es3002986.

Mishra, S. K., and S. N. Tripathi (2008), Modeling optical properties of mineral dust over the Indian Desert, *J. Geophys. Res.*, *113*, D23201, doi:10.1029/2008JD010048.

Miyakawa, T., N. Takegawa, and Y. Kondo (2008), Photochemical evolution of submicron aerosol chemical composition in the Tokyo megacity region in summer, *J. Geophys. Res.*, *113*, D14304, doi:10.1029/2007JD009493.

Mohan, M., and S. Payra (2009), Influence of aerosol spectrum and air pollutants on fog formation in urban environment of megacity Delhi, India, *Environ. Monit. Assess.*, *151*(1–4), 265–277, doi:10.1007/s10661-008-0268-8.

Moore, K. F., D. E. Sherman, J. E. Reilly, and J. L. Collett (2004a), Drop size-dependent chemical composition in clouds and fogs. Part I. Observations, *Atmos. Environ.*, *38*(10), 1389–1402, doi:10.1016/j.atmosenv.2003.12.013.

Moore, K. F., D. E. Sherman, J. E. Reilly, M. P. Hannigan, T. Lee, and J. L. Collett (2004b), Drop size-dependent chemical composition of clouds and fogs. Part II: Relevance to interpreting the aerosol/trace gas/fog system, *Atmos. Environ.*, *38*(10), 1403–1415, doi:10.1016/j.atmosenv.2003.12.014.

Munger, J. W., D. J. Jacob, J. M. Waldman, and M. R. Hoffmann (1983), Fogwater chemistry in an urban atmosphere, *J. Geophys. Res.*, *88*(C9), 5109–5121, doi:10.1029/JC088iC09p05109.

Munger, J. W., C. Tiller, and M. R. Hoffmann (1986), Identification of hydroxymethanesulfonate in fog water, *Science*, *231*(4735), 247–249, doi:10.1126/science.231.4735.247.

Murphy, B., N. M. Donahue, and S. N. Pandis (2012), Simulating ambient organic aerosol aging with the 2D volatility basis set, *Abstr. Pap. Am. Chem. Soc.*, *243*.

Ng, N. L., M. R. Canagaratna, J. L. Jimenez, P. S. Chhabra, J. H. Seinfeld, and D. R. Worsnop (2011), Changes in organic aerosol composition with aging inferred from aerosol mass spectra, *Atmos. Chem. Phys.*, *11*(13), 6465–6474, doi:10.5194/acp-11-6465-2011.

Nguyen, T. B., P. B. Lee, K. M. Updyke, D. L. Bones, J. Laskin, A. Laskin, and S. A. Nizkorodov (2012), Formation of nitrogen- and sulfur-containing light-absorbing compounds accelerated by evaporation of water from secondary organic aerosols, *J. Geophys. Res.*, *117*, D01207, doi:10.1029/2011JD016944.

Paciga, A., et al. (2016), Volatility of organic aerosol and its components in the megacity of Paris, *Atmos. Chem. Phys.*, *16*(4), 2013–2023, doi:10.5194/acp-16-2013-2016.

Pandis, S. N., J. H. Seinfeld, and C. Pilinis (1990), Chemical composition differences in fog and cloud droplets of different sizes, *Atmos. Environ. Part A.*, *24*(7), 1957–1969, doi:10.1016/0960-1686(90)90529-V.

Pandithurai, G., T. Takamura, J. Yamaguchi, K. Miyagi, T. Takano, Y. Ishizaka, S. Dipu, and A. Shimizu (2009), Aerosol effect on cloud droplet size as monitored from surface-based remote sensing over East China Sea region, *Geophys. Res. Lett.*, *36*, L13805, doi:10.1029/2009GL038451.

Patidar, V., S. N. Tripathi, P. K. Bharti, and T. Gupta (2012), First surface measurement of cloud condensation nuclei over Kanpur, IGP: Role of long range transport, *Aerosol Sci. Technol.*, *46*, 973–982, doi:10.1080/02786826.2012.685113.

Perri, M. J., Y. B. Lim, S. P. Seitzinger, and B. J. Turpin (2010), Organosulfates from glycolaldehyde in aqueous aerosols and clouds: Laboratory studies, *Atmos. Environ.*, *44*(21–22), 2658–2664, doi:10.1016/j.atmosenv.2010.03.031.

Poulain, L., W. Birmili, F. Canonaco, M. Crippa, Z. J. Wu, S. Nordmann, G. Spindler, A. S. H. Prévôt, A. Wiedensohler, and H. Herrmann (2014), Chemical mass balance of 300°C non-volatile particles at the tropospheric research site Melpitz, Germany, *Atmos. Chem. Phys.*, *14*(18), 10,145–10,162, doi:10.5194/acp-14-10145-2014.

Raja, S., et al. (2008), Fog chemistry in the Texas-Louisiana Gulf Coast corridor, *Atmos. Environ.*, *42*(9), 2048–2061, doi:10.1016/j.atmosenv.2007.12.004.

Seinfeld, J. H., and S. N. Pandis (2006), *Atmospheric Chemistry and Physics: From Air Pollution to Climate Change*, 2nd ed., Wiley, Sussex.

Siefert, R. L., S. M. Webb, and M. R. Hoffmann (1996), Determination of photochemically available iron in ambient aerosols, *J. Geophys. Res.*, *101*(D9), 14,441–14,449, doi:10.1029/96JD00857.

Siefert, R. L., A. M. Johansen, M. R. Hoffmann, and S. O. Pehkonen (1998), Measurements of trace metal (Fe, Cu, Mn, Cr) oxidation states in fog and stratus clouds, *J. Air Waste Manage. Assoc.*, *48*, 128–143.

Singh, V. P., T. Gupta, S. N. Tripathi, C. Jariwala, and U. Das (2011), Experimental study of the effects of environmental and fog condensation nuclei parameters on the rate of fog formation and dissipation using a new laboratory scale fog generation facility, *Aerosol Air Qual. Res.*, *11*(2), 140–154, doi:10.4209/aaqr.2010.08.0071.

Sinha, V., V. Kumar, and C. Sarkar (2014), Chemical composition of pre-monsoon air in the Indo-Gangetic Plain measured using a new air quality facility and PTR-MS: High surface ozone and strong influence of biomass burning, *Atmos. Chem. Phys.*, *14*(12), 5921–5941, doi:10.5194/acp-14-5921-2014.

Sorooshian, A., Z. Wang, M. M. Coggon, H. H. Jonsson, and B. Ervens (2013), Observations of sharp oxalate reductions in stratocumulus clouds at variable altitudes: Organic acid and metal measurements during the 2011 E-PEACE campaign, *Environ. Sci. Technol.*, *47*(14), 7747–7756, doi:10.1021/es4012383.

Syed, F. S., H. Körnich, and M. Tjernström (2012), On the fog variability over South Asia, *Clim. Dyn.*, *39*(12), 2993–3005, doi:10.1007/s00382-012-1414-0.

Takegawa, N., Y. Miyazaki, Y. Kondo, Y. Komazaki, T. Miyakawa, J. L. Jimenez, J. T. Jayne, D. R. Worsnop, J. D. Allan, and R. J. Weber (2005), Characterization of an Aerodyne Aerosol Mass Spectrometer (AMS): Intercomparison with other aerosol instruments, *Aerosol Sci. Technol.*, *39*(8), 760–770, doi:10.1080/02786820500243404.

Tilgner, A., P. Brauer, R. Wolke, and H. Herrmann (2013), Modelling multiphase chemistry in deliquescent aerosols and clouds using CAPRAM3.0i, *J. Atmos. Chem.*, *70*(3), 221–256, doi:10.1007/s10874-013-9267-4.

Timonen, H., et al. (2013), Characteristics, sources and water-solubility of ambient submicron organic aerosol in springtime in Helsinki, Finland, *J. Aerosol Sci.*, *56*, 61–77, doi:10.1016/j.jaerosci.2012.06.005.

Tiwari, S., S. Payra, M. Mohan, S. Verma, and D. S. Bisht (2011), Visibility degradation during foggy period due to anthropogenic urban aerosol at Delhi, India, *Atmos. Pollut. Res.*, *2*(1), 116–120, doi:10.5094/APR.2011.014.

Tritscher, T., et al. (2011), Volatility and hygroscopicity of aging secondary organic aerosol in a smog chamber, *Atmos. Chem. Phys.*, *11*(22), 11,477–11,496, doi:10.5194/acp-11-11477-2011.

Washenfelder, R. A., et al. (2011), The glyoxal budget and its contribution to organic aerosol for Los Angeles, California, during CalNex 2010, *J. Geophys. Res.*, *116*, D00V02, doi:10.1029/2011JD016314.

Weller, C., A. Tilgner, P. Braeuer, and H. Herrmann (2014), Modeling the impact of iron-carboxylate photochemistry on radical budget and carboxylate degradation in cloud droplets and particles, *Environ. Sci. Technol.*, *48*(10), 5652–5659, doi:10.1021/es4056643.

Whiteaker, J. R., and K. A. Prather (2003), Hydroxymethanesulfonate as a tracer for fog processing of individual aerosol particles, *Atmos. Environ.*, *37*(8), 1033–1043, doi:10.1016/s1352-2310(02)01029-4.

Xu, J. Z., Q. Zhang, Z. B. Wang, G. M. Yu, X. L. Ge, and X. Qin (2015), Chemical composition and size distribution of summertime PM 2.5 at a high altitude remote location in the northeast of the Qinghai–Xizang (Tibet) Plateau: Insights into aerosol sources and processing in free troposphere, *Atmos. Chem. Phys.*, *15*(9), 5069–5081, doi:10.5194/acp-15-5069-2015.

Yu, L., J. Smith, A. Laskin, C. Anastasio, J. Laskin, and Q. Zhang (2014), Chemical characterization of SOA formed from aqueous-phase reactions of phenols with the triplet excited state of carbonyl and hydroxyl radical, *Atmos. Chem. Phys.*, *14*(24), 13,801–13,816, doi:10.5194/acp-14-13801-2014.

Zhang, Q., M. R. Alfarra, D. R. Worsnop, J. D. Allan, H. Coe, M. R. Canagaratna, and J. L. Jimenez (2005), Deconvolution and quantification of hydrocarbon-like and oxygenated organic aerosols based on aerosol mass spectrometry, *Environ. Sci. Technol.*, *39*(13), 4938–4952, doi:10.1021/es048568l.

Zhao, R., A. K. Y. Lee, R. Soong, A. J. Simpson, and J. P. D. Abbatt (2013a), Formation of aqueous-phase alpha-hydroxyhydroperoxides (alpha-HHP): Potential atmospheric impacts, *Atmos. Chem. Phys.*, *13*(12), 5857–5872, doi:10.5194/acp-13-5857-2013.

Zhao, Y., A. G. Hallar, and L. R. Mazzoleni (2013b), Atmospheric organic matter in clouds: Exact masses and molecular formula identification using ultrahigh-resolution FT-ICR mass spectrometry, *Atmos. Chem. Phys.*, *13*(24), 12,343–12,362, doi:10.5194/acp-13-12343-2013.